Gamow-Teller transitions
- a key to open a jewel box of nuclear physics -

Yoshitaka Fujita
Department of Physics, Osaka University, Toyonaka, Osaka 560-0043, Japan
E-mail: fujita@rcnp.osaka-u.ac.jp

Abstract
The Gamow-Teller (GT) transitions, due to the simplicity of the $\sigma\tau$ operator that causes them, are more sensitive to the nuclear structures of initial and final states than any other transitions. A high energy-resolution achieved in the $(^3\mathrm{He}, t)$ charge-exchange reaction at 0° and at an intermediate beam energy of 140 MeV/nucleon started to show the details of fine structures and thus various unique features of GT transitions.

1 Introduction

Gamow-Teller (GT) transitions are associated with the simple $\sigma\tau$ operator with $\Delta L = 0$ nature [1]. As a consequence, there come out some of the important and unique features. In GT transitions, we find that
(1) states with similar spatial shapes are favorably connected,
(2) due to the σ operator, states having the $j_>(= \ell + 1/2)$ and/or $j_<(= \ell - 1/2)$ configurations as components can be connected, and
(3) due to the τ operator, in combination with the σ operator, the isospin quantum number T plays an important role.

The names "Gamow-Teller" and also "Fermi" come from the "allowed transitions" in β decay. Since β decays favor $\Delta L = 0$ transitions, they can study the GT and Fermi transitions clearly. There, the partial half-life t_i of the ith GT transition and t_F of the Fermi transition multiplied by the phase-space factor (f-factor) are related to the GT transition strength B(GT) and the Fermi transition strength B(F),

$$f_i t_i = K/\lambda^2 B_i(\mathrm{GT}) \quad \text{and} \quad f_\mathrm{F} t_\mathrm{F} = K/B(\mathrm{F})(1-\delta_c), \tag{1}$$

where $K = 6147.8(16)$, $\lambda = g_A/g_V = -1.270(3)$, δ_c is the Coulomb correction factor [2], and f_F and f_i are the phase-space factors (f-factors) of the β decay to the isobaric analog state (IAS) and to the ith GT state, respectively. The f-factor becomes smaller if the decay Q value is smaller. Therefore, the decays to higher excited states are suppressed.

Charge-exchange (CE) reactions, including $(^3\mathrm{He}, t)$ reaction, allow access to transitions to higher excited states. At intermediate energies ($\geq$ 100 MeV/nucleon) and at forward angles including 0°, GT states are prominent in CE reactions, because of their $L = 0$ nature and the dominance of the $\sigma\tau$ part of the effective nucleon-nucleon interaction at small momentum transfer q [3]. It was shown that they are good probes of GT transitions due to the fact that there is a simple proportionality between the GT cross sections at 0° and the B(GT) values [4]

$$\sigma_i^\mathrm{GT}(0^\circ) = \hat{\sigma}^\mathrm{GT}(0^\circ) B_i(\mathrm{GT}), \tag{2}$$

where $\hat{\sigma}^\mathrm{GT}(0^\circ)$ is the unit GT cross section at 0°, which depends on the mass A of the system and gradually decreases as a function of excitation energy [4]. Because of this proportionality, the study of B(GT) values can reliably be extended up to high excitations by using the "standard B(GT) values" that can be available from β decays [5].

2 High Resolution (^{3}He, t) Reaction at 0°

Studies of GT strengths by the β^--type (p, n) reaction started in the 1980s using proton beams at intermediate energies. They provided rich information on the overall GT strength distributions up to the energy region of the GT giant resonances (GT-GR) having their center at $E_x \approx 8 - 15$ MeV [6]. However, individual transitions were poorly studied due to the limited energy resolution (≈ 300 keV) in (p, n) reactions. Therefore, it was not easy to calibrate the unit cross section $\hat{\sigma}^{\rm GT}(0^\circ)$ by using standard B(GT) values from β-decay studies on a level-by-level base [4].

The development in full beam matching techniques [7–10] realized an energy resolution of ≈ 30 keV in (^{3}He, t) reactions at an intermediate energy of 140 MeV/nucleon and 0°. With this one order-of-magnitude better resolution, we can now study GT and Fermi states that were unresolved in the pioneering (p, n) reactions (see Fig. 1). The validity of the proportionality [Eq. (2)] was examined by comparing the GT transition strengths in the (^{3}He, t) spectra to the B(GT) values from mirror β decays. Good proportionality of $\approx 5\%$ was demonstrated for "$L = 0$" transitions with $B(\mathrm{GT}) \geq 0.04$ in studies of the $A = 26$, 27 and 34 nuclear systems [12–15].

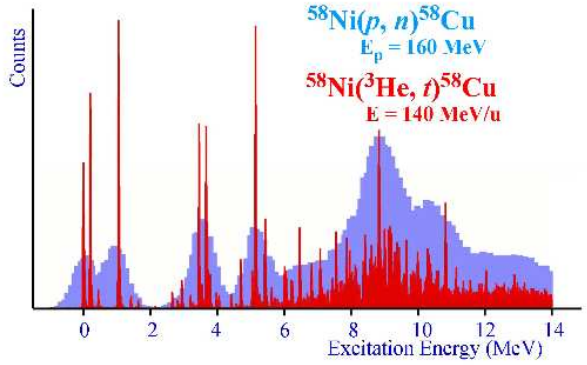

Fig. 1: Energy spectra of charge-exchange reactions at 0°. The broad spectrum is from ^{58}Ni$(p, n)^{58}$Cu reaction measured in 1980's [6]. In the recent ^{58}Ni(^{3}He, t)^{58}Cu reaction [11] fine structure and sharp states have been observed up to the excitation energy of 13 MeV. The proton separation energy (S_p) is at 2.87 MeV. A increase of continuum is observed above $E_x = 6$ MeV.

In a few specific transitions, however, larger deviations $(20 - 40\%)$ from the proportionality were observed [15, 16]. The DWBA calculations performed using the transition matrix elements from shell-model calculations showed that the contribution of the Tensor interaction is responsible for these deviations from proportionality. It was found that in these cases two major $\Delta L = 0$ configurations, each of them having a large $\sigma\tau$ matrix element, contribute destructively to the GT transition strength. Then, the contribution of the $\Delta L = 2$ configurations activated by the $T\tau$ interaction is not negligible [15].

Owing to the high energy-resolution and the close proportionality given by Eq. (2), the (^{3}He, t) reaction is recognized as an excellent tool for the study of the GT transitions in nuclei, especially of the strengths to discrete states. In addition, one obtains information on the widths of the discrete states.

3 Observation of isospin and shape selection rules

It was thought that a low energy-resolution was sufficient for the study of light nuclei due to the low level-density. However, the possibility of studying decay widths changed this perception. An interesting example is the observation of a sharp state at $E_x \approx 15$ MeV in the ^{9}Be(^{3}He, t)^{9}B spectrum. This is a $T_z = +1/2 \rightarrow -1/2$ transition. In CE spectra taken in the past, a very simple structure consisting of a sharp $J^\pi = 3/2^-$ ground state (g.s.) and a broader 2.36 MeV state on top of a few-MeV-wide bump-like structure was identified, just as we see in Fig. 2(a). In ^{9}B, all states are situated above the proton and α separation energies of $S_p = -0.186$ MeV and $S_\alpha = -1.689$ MeV, respectively [17]. Therefore, thinking of the uncertainty principle, it was expected that states should have large widths [18].

By magnifying the vertical scale [see Fig. 2(b)], we can see a sharp state at $E_x = 14.66$ MeV. A high sensitivity accompanied by a high energy-resolution of about 30 keV was essential to observe this weakly excited state on top of the continuum. We found that the sharpness of the state can be explained

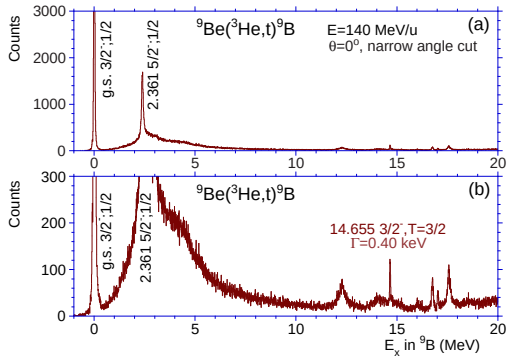

Fig. 2: The ^{9}Be(^{3}He, t)^{9}B spectrum in two vertical scales. (a) Simple structure as shown in this figure was identified in earlier CE reactions. (b) By magnifying the vertical scale by one order-of-magnitude, a weak, but sharp state is observed at $E_x = 14.66$ MeV.

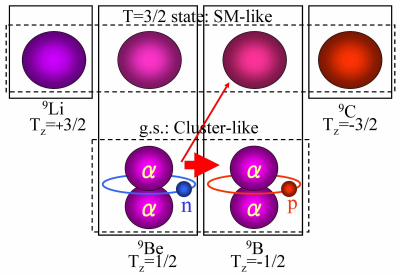

Fig. 3: ^{9}Be and ^{9}B are mirror nuclei having $T_z = +1/2$ and $-1/2$, respectively. It is suggested that g.s. of them have the main structure of 2α + one-nucleon. On the other hand, the $E_x = 14.66$ MeV, $T = 3/2$ state in ^{9}B is the IAS of the g.s. of ^{9}Li and ^{9}C having a spherical shape [19]. It should be noted that ^{9}Li and ^{9}C are the $p_{3/2}$ closed-shell nuclei.

by the isospin selection-rule that prohibits proton (and also α) decay. It is known that this 14.66 MeV state has an isospin value of $T = 3/2$, and is the IAS of the g.s. of ^{9}Li and ^{9}C [17]. The proton decay of ^{9}B results in ^{8}Be (actually two α particles). The nucleus ^{8}Be and the proton have isospin values of $T = 0$ and $1/2$, respectively. The vector sum of these two isospin values cannot form an isospin value of $3/2$; thus the proton decay is forbidden and the state is kept sharp. A recent analysis showed that several sharp states observed above 10.8 MeV in the ^{58}Ni(^{3}He, t)^{58}Cu reaction (see Fig. 1) have $T = 2$ [11]. Although these $T = 2$ states are located at nearly 10 MeV above the S_p value of 2.87 MeV, the proton decay into ^{57}Ni ($T_z = +1/2$, and thus the g.s. has $T = 1/2$) and a proton ($T = 1/2$) is not allowed.

It is known that both the g.s. and this 14.66 MeV state in ^{9}B have $J^\pi = 3/2^-$. Thus, they can be connected by an allowed GT transition with the $J^\pi = 3/2^-$ g.s. of ^{9}Be. However, in reality, the transition strengths differ by two orders-of-magnitude. It should be noted that the GT ($\sigma\tau$) operator cannot connect the states with different spatial shapes. Therefore, it is suggested that the g.s. of ^{9}Be (and of ^{9}B) have a different structure from the 14.66 MeV state in ^{9}B, which is the IAS of the g.s. of ^{9}Li and ^{9}C (see Fig. 3). In a recent calculation using the method of antisymmetrized molecular dynamics (AMD), a structure consisting of 2α + one-nucleon was predicted for the g.s. of ^{9}Be and ^{9}B, while a mean-field like structure is predicted for the 14.66 MeV state in ^{9}B and its IASs [19]. A detailed analysis for a spectrum with higher statistics is in progress [20].

3.1 GT transitions in the deformed $T = 1/2$ nuclei in the middle of sd shell

The spectra in Fig. 4 show the strength of the $T_z = +1/2 \rightarrow -1/2$ Fermi and GT transitions starting from the g.s. of ^{23}Na and ^{25}Mg target nuclei to the g.s. and the excited GT states in the mirror nuclei ^{23}Mg and ^{25}Al. As seen, the features of spectra are largely different in the low-lying region below $E_x = 6$ MeV. We see many prominent GT states in the $A = 23$ system [21], while the number of well-excited states is very few in the $A = 25$ system [22]. It is known that these nuclei are deformed in a prolate shape (deformation parameter $\delta \approx 0.4 - 0.5$). Therefore, we can assume that low-lying states of these nuclei have a structure of deformed (and rotating) core and a single nucleon. In largely deformed nuclei, each single nucleon is in a Nilsson orbit labeled by the asymptotic quantum numbers [23]. When the rotation of the core is perpendicular to the z axis, the z component K of the total spin J become an important quantum number. Therefore, the selection rules of $\Delta K = 0$ and ± 1, in addition to the usual selection rules of $\Delta J = 0$ and ± 1, should be taken into account [22, 23]. Each rotational band is specified by the quantum numbers of the single particle orbit $K^\pi[Nn_z\Lambda]$, where N is the total oscillator quantum number, n_z the number of quanta along the z axis and Λ is the z-axis projections of the orbital angular momentum.

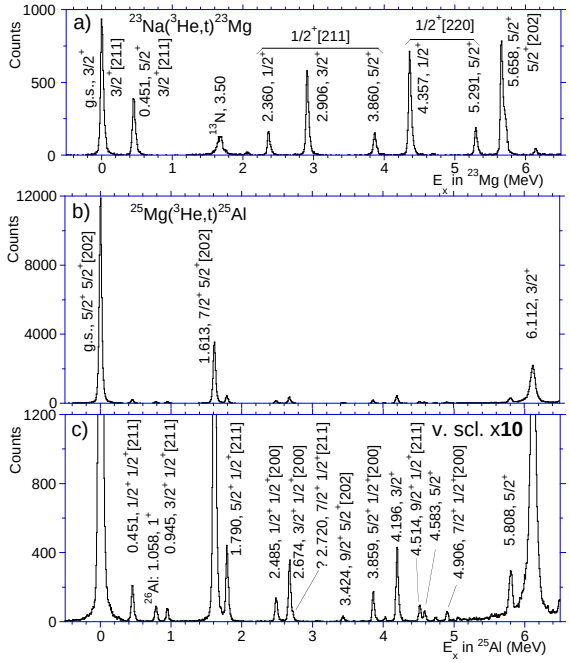

Fig. 4: Comparison of (a) ^{23}Na(^{3}He, t)^{23}Mg spectrum and (b) ^{25}Mg(^{3}He, t)^{25}Al spectrum. The ordinates of the figure (a) and (b) are scaled so that states with similar B(GT) values have similar peak heights. The vertical scale of ^{25}Mg(^{3}He, t)^{25}Al spectrum is expanded by a factor of ten in the figure (c) in order to show weakly excited states more clearly.

The ground states of the $A = 23$ mirror nuclei ^{23}Na and ^{23}Mg are specified by the quantum numbers $3/2^+[2\,1\,1]$ [see Fig. 4(a)]. Therefore, the transitions to the $K^\pi = 1/2^+, 3/2^+$ and $5/2^+$ bands are allowed by the K-selection rule. Note that each Nilsson orbit specified by the asymptotic quantum numbers is filled with two nucleons. Therefore, the increase of mass number A by 2 will change the configuration of the g.s. The ground states of the $A = 25$ mirror nuclei ^{25}Mg and ^{25}Al are specified by $5/2^+[2\,0\,2]$. Therefore, the transitions from the ground states to the states of the common $1/2^+[2\,1\,1]$ band, for example, have different natures of $\Delta K = 1$ and 2 in the $A = 23$ and $A = 25$ systems, respectively. Those transitions that were allowed in the $A = 23$ system, therefore, are not anymore allowed in the $A = 25$ system.

An interesting feature that became apparent from the comparison of these $A = 23$ and 25 systems is that at the deformation $\delta \approx 0.4 - 0.5$ the K selection rules are superior to the selection rules of asymptotic quantum numbers that would work first for very large axially-symmetric quadrupole deformation. One can point out that transitions from the ^{23}Na ground state of the $3/2^+[2\,1\,1]$ band to the 4.357 MeV, $1/2^+$ and 5.291 MeV, $5/2^+$ states of the $1/2^+[2\,2\,0]$ band in ^{23}Mg are, in principle, not allowed by the $\sigma\tau$ operator due to the $\Delta n_z = 1$ and $\Delta\Lambda = 1$ nature of these transitions. They, however, are rather strongly excited, as seen in Fig. 4(a), because these transitions are allowed in terms of the K selection rule. Similarly, the transition to the 5.658 MeV, $5/2^+$ state of the $5/2^+[2\,0\,2]$ band is rather strong. We see that this transition is allowed by the K-selection, but not allowed by the n_z and Λ selections [22].

4 Development of Giant Resonance Structure in pf-shell Nuclei

In nuclei lighter than sd-shell, we hardly see a prominent giant-resonance structure of GT transitions. However, in nuclei heavier than nickel (mass $A \geq 58$), we usually see well developed GT-GRs [6]. Therefore, it is expected that we can observe the development of the GT-GR structure for the nuclei in the f-shell region.

The main configurations of the GT-GRs of usual $N > Z$ nuclei are of p-h nature. The observation of a GT-GR at much higher E_x ($\approx 8 - 15$ MeV) than the energy gap of $j_<$ and $j_>$ orbits ($\approx 3 - 6$ MeV) can be partly explained by the repulsive nature of the p-h interaction [24]. In addition, IV-type interactions are repulsive. Therefore, the GR structure in the IV-type GT excitations can be pushed up further.

However, in light $f_{7/2}$-shell nuclei we notice that GT excitations with pure p-p configurations can be realized as a rare case due to the CE nature of the excitation and also due to the fact that only two configurations consisting of $f_{7/2}$ orbit with the $j_>$ nature and $f_{5/2}$ orbit with the $j_<$ nature can contribute to the GT transitions. Then, there comes out a naive question how the attractive p-p (or h-h) interaction competes with the repulsive p-h interaction in the IV-type GT excitation.

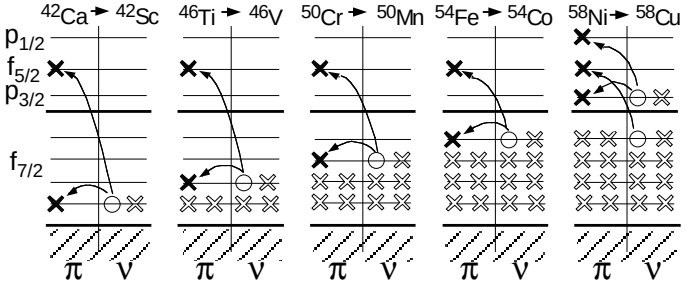

Fig. 5: Allowed configurations of GT$_-$ transitions starting from $T_Z = +1$ to $T_Z = 0$ nuclei in the pf-shell, where most simplified shell structure is assumed. The filling of protons (π) and neutrons (ν) are shown by open crosses. The newly created holes and particles after the transitions are shown by the open circles and filled crosses, respectively.

We find that such a competition can be ideally studied by examining the mass dependence of the GT strength distribution starting from the $N = Z+2$ ($T_z = 1$) even-even $f_{7/2}$-shell nuclei to the $N = Z$ ($T_z = 0$) odd-odd nuclei, where T_z, defined by $(N - Z)/2$, is the z component of isospin T. We can study for $A = 42, 46, 50$ and 54 systems, where initial nuclei are ^{42}Ca, ^{46}Ti, ^{50}Cr and ^{54}Fe, respectively. As A increases, the $f_{7/2}$ orbit will be filled gradually on top of the $Z = N = 20$, ^{40}Ca inert core while the $f_{5/2}$ orbit is always kept open (see Fig. 5).

Since the initial and final T_z values are identical for all cases, it is expected that the total GT strengths are not so different [25]. In addition, the strength distribution is not affected by the isospin Clebsch-Gordan coefficients that re-distribute the GT strength among the final $T = T_0 - 1$, T_0 and $T_0 + 1$ states [11, 26] with T_0 being the isospin of the initial state.

In these nuclei, the GT excitations all have the same nature of $\nu f_{7/2} \rightarrow \pi f_{7/2}$ and $\nu f_{7/2} \rightarrow \pi f_{5/2}$. However, in the $A = 42$ system, we notice that the two final configurations, i.e., both $(\pi f_{7/2}, \nu f_{7/2})$ and $(\pi f_{5/2}, \nu f_{7/2})$, have attractive p-p nature. As A increases, the latter looses its p-p nature and tends to have the repulsive p-h nature, as is clear in the $A = 54$ system (see Fig. 5). The former also looses its p-p nature, but in $A = 54$ it again has the attractive h-h nature. In the $A = 58$ system, the p-p type $(\pi p_{3/2}, \nu p_{3/2})$ and $(\pi p_{1/2}, \nu p_{3/2})$ configurations further take part in, and additional conflict with the repulsive $(\pi f_{5/2}, \nu f_{7/2})$, p-h configuration is expected.

With the splendid resolutions of $25 - 40$ keV, the GT strength distributions of the transitions starting from the $T_z = +1$ target nuclei with $A = 42 - 58$ were studied in detail as shown in Fig. 6 [5, 27,28]. The analysis of the angular distribution for each transition suggested that most of the well excited states have the $L = 0$ nature and they are the GT excitations. We see that the Gamow-Teller (GT) strength that is concentrated in one low-lying state in the lightest odd-odd $N = Z$ f-shell nucleus ^{42}Sc moves up to higher energy region with the increase of mass A and finally forms a GR structure in the heaviest f-shell nucleus ^{54}Co and also in ^{58}Cu.

From Fig. 6, it is clear that the GT strengths in ^{42}Sc are pulled down and accumulated to the 0.61 MeV, 1^+ state. This feature can be explained by the fact that both $(\pi f_{7/2}, \nu f_{7/2})$ and $(\pi f_{5/2}, \nu f_{7/2})$ configurations have the attractive p-p nature in ^{42}Sc (see Fig. 5). On the other hand in ^{54}Co, in which the $(\pi f_{5/2}, \nu f_{7/2})$ configuration has clearly the repulsive p-h nature, the main part of the GT strength is pushed up. The $(\pi f_{7/2}, \nu f_{7/2})$ configuration has the attractive h-h nature, but only 10 to 15 % of the observed GT strength remains in the first 1^+ state. The overall repulsive nature of the residual interaction in ^{54}Co can be understood by the numbers of available transitions that make the $(\pi f_{5/2}, \nu f_{7/2})$, p-h configuration and the $(\pi f_{7/2}, \nu f_{7/2})$, h-h configuration; assuming a simple shell structure, they are 48 and 16, respectively. In ^{58}Cu, due to the additional $(\pi p_{3/2}, \nu p_{3/2})$ and $(\pi p_{1/2}, \nu p_{3/2})$ configurations, strengths are also observed at $E_x = 3 - 5$ MeV. However, the dominance of the repulsive p-h type

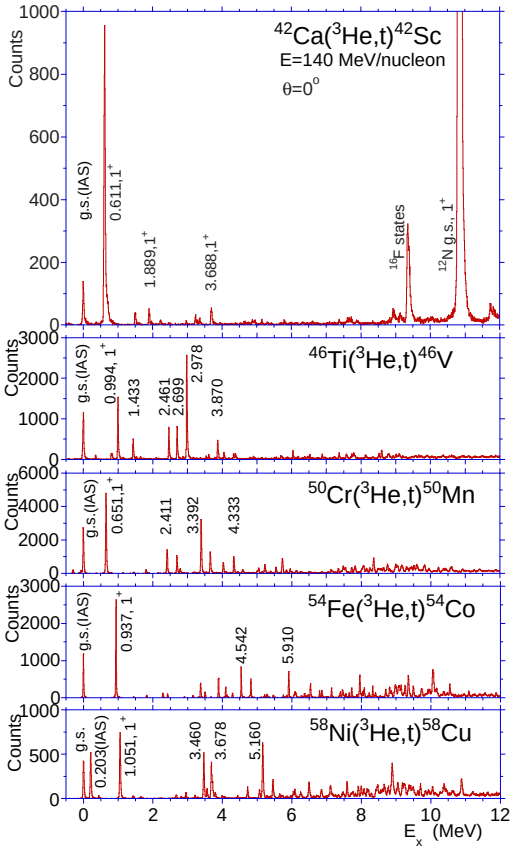

Fig. 6: High energy-resolution $(^3\mathrm{He}, t)$ spectra for $T_z = +1$ target nuclei in the pf shell. An energy resolution of ≈ 30 keV is obtained. The result of the angular distribution suggests that most of the prominent states are $L = 0$ GT states. The vertical scale is normalized by the heights of the IAS peaks all having $B(\mathrm{F}) = 2$. Thus, peak heights are almost proportional to B(GT). As the mass number A increases, the GT states are more fragmented and more GT strength is found in a higher energy region of $7 - 12$ MeV.

$(\pi f_{5/2}, \nu f_{7/2})$ configuration still pushes the main part of the GT strength to the higher E_x region.

It is now clear that the repulsive nature of the p-h type configurations mainly contribute to the formation of the GR structures in nuclei. In CE reactions, however, p-p type configurations can also be realized as a rare case. In such cases the GT strengths are concentrated to the transition to the lowest-lying GT state, as we have seen in the ^{42}Ca$(^3\mathrm{He}, t)^{42}$Sc measurement. The logft value of the mirror GT transition that has been studied in the ^{42}Ti β-decay to the 0.61 MeV, 1^+ state is as small as 3.18(11), a value similar with the super-allowed Fermi transition. Therefore, we suggest that this strong GT transition is called by the name "super-allowed GT transition", and the 0.61 MeV, 1^+ state "super-allowed GT state."

Other examples of the super-allowed GT transitions are the g.s.$-$g.s. GT transition of the ^{18}Ne β^+) decay to ^{18}F, and the g.s.$-$g.s. GT transition of the ^{6}He β^- decay to ^{6}Li. They have the logft values of 3.1 and 2.9, respectively. It should be noted that all of these final states have the p-p type configurations on top of the doubly LS-closed shell structure, i.e., the structure of the super-allowed GT state.

5 Gamow-Teller Resonance Structures in ^{118}Sb

As shown in Fig. 1, the broad bump-like structure of GT-GRs observed in ^{58}Ni$(p, n)^{58}$Cu reaction measured in 1980's [6] was resolved into fine structure and sharp states in the recent ^{58}Ni$(^3\mathrm{He}, t)^{58}$Cu measurement [11]. It is then our interest whether such fine structures can be found even in heavier nuclei in the study using the high-resolution $(^3\mathrm{He}, t)$ reactions. The level density of GT states is another interest. We select ^{118}Sn as the target nucleus. It is a representative spherical medium-heavy nucleus.

The ^{118}Sn$(^3\mathrm{He}, t)^{118}$Sb spectrum taken at 0° with a resolution of 30 keV is shown in Fig. 7. The g.s. of ^{118}Sb has the $J^\pi = 1^+$, and the g.s.$-$g.s. transition starting from the 0^+ g.s. of ^{118}Sn is the GT transition. Since the B(GT) value of this transition is well determined in the β-decay study of ^{118}Sb, we can get the unit GT cross section $\hat{\sigma}^{\mathrm{GT}}(0^\circ)$. Then, using the Eq. 2, the B(GT) values can be deduced for the transitions to excited states. In this spectrum, the $E_x = 51$ keV, 3^+ state in ^{118}Sb was clearly

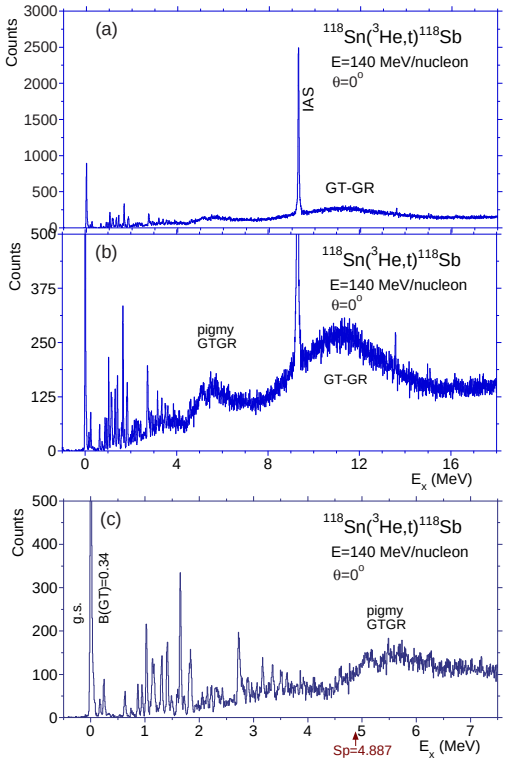

Fig. 7: (a) ^{118}Sn(^{3}He, t)^{118}Sb spectrum. Discrete ground state, low-lying states, and the IAS are prominent. (b) ^{118}Sn(^{3}He, t)^{118}Sb spectrum with an expanded vertical scale. (c) ^{118}Sn(^{3}He, t)^{118}Sb spectrum with an expanded vertical as well as energy scale.

recognized as a skirt of the g.s. peak, and we expect to get a reliable cross section for the g.s.−g.s. transition.

The proton separation energies S_p is $4.887(3)$ MeV in ^{118}Sb. Therefore, there should be no decay width for the excited states below this energy and we should see discrete states. We see that the low-lying states below $E_x = 2$ MeV are mostly well separated. In the energy region between $2 - 4$ MeV, however, we see fine structures, but the spectra are not decomposed into states even with our resolution of 30 keV. Taking our energy resolution of 30 keV, we suggest that the level density of the GT states in this region is higher than one per 30 keV at $E_x = 4$ MeV. Above this energy region, only the IAS has been clearly observed as discrete state. The IAS is apparently wider than the g.s., showing the spreading and decay width due to the isospin impurity in the IAS.

In ^{118}Sb, it is interesting to see that the GT strength is divided into four parts, i.e., the g.s., the clustering states in $E_x = 1 - 2$ MeV, $2 - 4$ MeV, a bump-like structure in $4 - 8$ MeV and the GT-GR structure in $E_x = 8 - 15$ MeV. The bump-like structure in $4 - 8$ MeV is called the pigmy GT resonance [29]. It is stressed that the existence of such an interesting structure even in a nucleus with a relatively high mass of $A = 118$ is a challenge to the understanding of nuclear structure.

The high-resolution (^{3}He, t) experiments were performed at RCNP, Osaka. The author is grateful to the participants of the experiments and the accelerator group of RCNP. This work was in part supported by Monbukagakusho, Japan under Grant No. 18540270 and by the Japan-Spain collaboration programme by JSPS. Discussions with B. Rubio (Valencia), I. Hamamoto (Lund), W. Gelletly (Surrey), P. von Brentano (Köln) and K. Muto (TIT) are acknowledged.

References

[1] F. Osterfeld, Rev. Mod. Phys. **64**, 491 (1992), and references therein.

[2] J.C. Hardy and I.S. Towner, Phys. Rev. C **71**, 055501 (2005), *ibid.* Nucl. Phys. News **16**, 11 (2006).

[3] W.G. Love and M.A. Franey, Phys. Rev. C **24**, 1073 (1981).

[4] T.N. Taddeucci *et al.*, Nucl. Phys. **A469**, 125 (1987).
[5] Y. Fujita *et al.*, Phys. Rev. Lett. **95**, 212501 (2005).
[6] J. Rapaport and E. Sugarbaker, Annu. Rev. Nucl. Part. Sci. **44**, 109 (1994).
[7] Y. Fujita *et al.*, Nucl. Instrum. Meth. Phys. Res. B **126**, 274 (1997); and references therein.
[8] Y. Fujita *et al.*, Nucl. Phys. **A687**, 311c (2001).
[9] H. Fujita *et al.*, Nucl. Instrum. Meth. Phys. Res. A **469**, 55 (2001).
[10] H. Fujita *et al.*, Nucl. Instrum. Meth. Phys. Res. A **484**, 17 (2002).
[11] H. Fujita *et al.*, Phys. Rev. C **75**, 034310 (2007).
[12] Y. Fujita *et al.*, Phys. Rev. C **67**, 064312 (2003).
[13] R. Zegers *et al.*, Phys. Rev. C **74**, 024309 (2006).
[14] Y. Fujita *et al.*, Phys. Rev. C **59**, 90 (1999).
[15] Y. Fujita *et al.*, Phys. Rev. C **75**, 057305 (2007).
[16] A.L. Cole *et al.*, Phys. Rev. C **74**, 034333 (2006).
[17] J.H. Kelley, C.G. Sheu, J.L. Godwin *et al.*, Nucl. Phys. **A745**, 155 (2004).
[18] Y. Fujita, Nucl. Phys. **A805**, 408c (2008).
[19] Y. Kanada-En'yo, YITP, Kyoto, private communication.
[20] C. Scholl, IKP, Köln, private communication.
[21] Y. Fujita *et al.*, Phys. Rev. C **66**, 044313 (2002).
[22] Y. Shimbara *et al.*, Eur. Phys. J. A **19**, 25 (2004).
[23] A. Bohr and B. Mottelson, *Nuclear Structure* (Benjamin, New York, 1975), Vol. 2.
[24] J.P. Schiffer and W.W. True, Rev. Mod. Phys. **48**, 191 (1996).
[25] M.N. Harakeh, A. Van Der Woude, *Giant Resonances* Oxford Studies in Nucl. Phys. 24 (Oxford University Press, Oxford, 2001).
[26] Y. Fujita *et al.*, Phys. Rev. C **62**, 044314 (2000).
[27] T. Adachi *et al.*, Phys. Rev. C **73**, 024311 (2006).
[28] T. Adachi *et al.*, Nucl. Phys. **A788**, 70c (2007).
[29] K. Pham *et al.*, Phys. Rev. C **51**, 526 (1995).